Thermodynamic, Kinetic and Equilibrium Investigation of Activated Carbon Prepared from the Bark of *Azadirachta indica L.* Acid Dispersion to Remove Congo Red Dye

A. Siva Kumar[1,2]*, G. Rama Chandran[3] and P. Thamilarasu[4]
[1]R & D Centre for Bharathiar University, Coimbatore, 641046, India
[2]Department of Chemistry, Rajah Serfoji Government College, Thanjavur, 613005, India
[3]Department of Chemistry, Dr.Ambedkar Govt Arts College, Vyasarpadi, Chennai, 600039, India
[4]Department of Chemistry, Arignar Anna Government Arts College, Namakkal, 637002, India
*Corresponding Author (e-mail: mietsivakumar@gmail.com)

The investigation studied the removal of Congo red dye in aqueous solutions via adsorption by *Azadirachta indica* L. Bark Activated Carbon (AIBAC) under a variety of experimental strategies and optimization circumstances. By using the adsorption equilibrium method, various parameters have been examined. Freundlich, Langmuir, and Temkin adsorption isotherms were employed to analyse the adsorption isotherm. Thermodynamic parameters such as ΔH^o, ΔS^o and ΔG^o were calculated, which indicated that the adsorption was spontaneous and endothermic. The kinetics of fictional second order was more appropriate than the pseudo-first order kinetic model. Through FTIR spectroscopy and SEM, AIBAC was examined both before and after the penetration of Congo red dye in water.

Keywords: Activated charcoal; Congo red dye; adsorption; isotherm; kinetic; thermodynamic study

Discharge of effluents, bearing dyes, surfactants, heavy metals, salts etc., from industries like paint, textile, tanneries, printing, electroplating etc. not only pollutes ground water and surface water, but also imparts toxicity and has no visibility; and recent statistics show that 12% of textile dyes used annually is wasted during production and processing operations, and that 30-35% of these input colours winds up in the environment through effluents produced by the treatment of residual industrial water [1, 2]. In the textile processing sector, colours are regularly given through pigments and colourants. After colouring, the excess water comes out as effluent, which is considered as a pollutant due to the toxicity. It causes cancer and respiratory problems. It changes the appearance of water, making water more disagreeable on aesthetic grounds, and obstructs the transmission of biological processes that would otherwise protect aquatic communities in ecosystems, and induces micro-toxicity at high levels [2, 3]. Therefore, it is challenging to forecast the toxicity of dyes in effluents in order to limit environmental contamination at its source. The toxicity of effluents might be estimated using fundamental dyeing characteristics such as shade depth, cloth weight, and colour production caused by sulphur dyes, such as fixing. The outcomes of these forecasts are satisfactory, and this knowledge is beneficial to industries; harmful effects of dyes for waste reduction by choosing low dye concentrations in the process [4]. To lessen the effects of industrial effluents on the environment, a variety of techniques have been examined for the purpose of colour removal. These techniques include photo-oxidation, photo-catalysis, ozonation, coagulation, and chemical oxidation [5-8], as well as adsorption on inorganic (or organic) matrices and microbiological decomposition [9]. Among the techniques, the most favoured method of removing dyestuff from effluents or municipal wastewater is adsorption. The high cost of currently available commercially-used adsorbents is the main obstacle to enterprises using this technology. If the adsorbents are inexpensive, the cost of adsorption technology would also decrease. As a result, more affordable alternatives have been suggested; including waste coir pith[10], *Parthenium hysterophorus* [11], pine sawdust [12, 14], granulated sugar [13], rubber wood sawdust [15], de-oiled soya and bottom-up ash [16], palm kernel [17], crow feathers [18], etc. Based on the aforementioned analysis of the literature, it was decided to employ *Azadirachta indica* L. Bark Activated Carbon (AIBAC), a cheap and readily available adsorbent material that can effectively remove Congo red dye (CRD) using water-based treatments.

MATERIALS AND METHODS

1. Materials

Azadirachta indica L. Bark Activated Carbon was employed to perform as an adsorbent to bind to

39   A. Siva Kumar, G. Rama Chandran, and P. Thamilarasu

Thermodynamic, Kinetic and Equilibrium Investigation of Activated Carbon Prepared from the Bark of *Azadirachta indica L.* Acid Dispersion to Remove Congo Red Dye

Congo red dye in aqueous solutions. Each and every reagent used this investigation is widely accessible from suppliers (E-Merck and SD-fine, India).

2.   Process of Making Activated Carbon

Activated carbon was prepared from the bark of *Azadirachta indica L.* and the base material was obtained from a local supplier of basic materials. After being cut into small pieces and dried, the material was rinsed in hot distilled water (60°C) to get rid of any traces of dirt. Then, concentrated H_2SO_4 was used to impregnate the base material. A ratio of 0.5:1 of material weight to acid volume was used for impregnation. The roasted substance was then repeatedly washed with plain water till the pH of the wash water reached neutral. A muffle furnace was employed to carbonise the material after it had been dried at 500^0C. It was finally crushed and sieved before being transformed into activated carbon.

3.   Adsorption Studies

Dye solutions consisting of 1000 mg/L of dye dissolved in known amounts of water were prepared. Two stock solutions of Congo red dye (CRD) in distilled water were used throughout the study. Throughout the study, double-distilled water was used. By employing the training set methodology, adsorption tests were done. Iodine flasks with 100 mg of adsorbent and 100 ml of CRD of known concentrations were prepared. The contents were then homogenised in a temperature-controlled water bath (Techno) at different intervals. The concentration of Congo red dye was determined using a spectrophotometer calibrated at 497 nm. The solutions were shaken at regular intervals and the filtrate was always present. The experiments were repeated at various temperatures to absorb CRD from the aqueous solutions, in particular at 30°C, 40°C, and 50°C [19].

The formula below was used to calculate adsorption capacity:

$$\text{Adsorption capacity}\quad q_e = \frac{(C_o - C_e)}{W}\,V \qquad (1)$$

Where C_o represents the initial concentration (mg/L) of the CRD solution, C_e represents the final concentration (mg/L) of the CRD solution, V represents the volume (mL) of the CRD solution, and W represents the weight (g) of AIBAC (g).

RESULTS AND DISCUSSION

1.   Effects of Amount of Adsorbent, Time, pH, and Concentration

The amount of adsorbent used for the aforementioned tests ranged from 50 to 300 mg. 100 ml of well-shaken mixture containing 10 mg/L of Congo red dye solution was used at random times. The findings demonstrated that in order to remove CRD the most, the optimal amount of adsorbent was established at 100 mg, the optimal agitation period at 100 min, and the optimal pH at 5.0.

2.   Discernment of Temperature and Initial Concentration

The time at equilibrium was independent of initial CRD concentration (C_o). The findings, as presented in Table 1, confirmed that amount of CRD adsorbed (q_e) increases by a reduction in percentage of removal, while initial concentration of CRD increases, due to comparatively higher driving force of mass transfer. Aqueous solution to solid media mass transfer resistance is largely overcome by initial concentration [20]. From 30°C to 50°C, the proportion of CRD elimination increased. The process of adsorption endothermic character was demonstrated.

Table 1. Optimal conditions and elimination of CRD from AIBAC.

Initial conc. of CRD (C_o) mg/L	Equilibrium Conc. of CRD (C_e), mg/L			Amount of CRD adsorbed at equilibrium (q_e), mg/g			CRD exclusion (%) by AIBAC		
	30°C	40°C	50°C	30°C	40°C	50°C	30°C	40°C	50°C
10	2.064	1.605	1.147	7.936	8.396	8.853	79.36	83.96	88.53
20	5.642	5.138	4.220	14.358	14.862	15.780	71.79	74.31	78.90
30	10.596	8.991	7.844	19.404	21.009	22.156	64.68	70.03	73.85
40	16.835	15.917	13.624	23.165	24.083	26.376	57.91	60.21	65.94
50	23.073	23.578	21.651	26.927	26.422	28.349	53.85	52.84	56.70

40   A. Siva Kumar, G. Rama Chandran,
and P. Thamilarasu

Thermodynamic, Kinetic and Equilibrium Investigation of
Activated Carbon Prepared from the Bark of *Azadirachta
indica L.* Acid Dispersion to Remove Congo Red Dye

3.   Adsorption Isotherms

The Tempkin, Freundlich, and Langmuir isotherm systems were employed to analyse the colourant. Dispersal in the fluid and rock-solid phases with the optimum correlation between adsorbate concentration (C_e) and adsorption capacity (q_e) in the bulk fluid phase was shown [21].

The reorganised Langmuir model's linear form is provided as follows, in reference to [20].

$$\frac{C_e}{q_e} = \frac{1}{Q_0 . b_L} + \frac{C_e}{Q_0} \quad (2)$$

Based on the plot's slope and intercept (C_e) / (q_e) vs., the constants Q_0 and b_L could be computed.

The Freundlich equation's linear version is as the following [22].

$$\log q_e = \log k_f + \frac{1}{n} \log C_e \quad (3)$$

The Langmuir constants Q_o and b_L pertain to the monolayer adsorption capability (mg / g), as well as adsorption energy (L / mg), and q_e and n try to compensate the Freundlich isotherm's empirical constants,; measuring the adsorption capacity (mg^{-1} 1/n L$_1$/ m g$^{-1)}$) and the adsorption force, respectively. C_e stands for the final concentration of CRD in the solution. C_e / q_e vs C_e in the Langmuir adsorption isotherm is shown in Figure 1, and log q_e versus log C_e in the Freundlich adsorption isotherm is shown in Figure 2.

Lower temperatures may be more favourable for adsorption, as seen by the monolayer adsorption capacity measurements (Q_o) rising with temperature. Because of how quickly the dye diffused into AIBAC at lower temperatures, this phenomenon can be explained. The adsorption energy (b_L) value suggests that the binding site's affinity with the dye is advantageous. As the temperature of the solution increased from 30°C to 50°C, adsorption capacity (k_f) values increased. This evidence suggests that high temperature promotes adsorption. As temperature increased, there were slight changes in adsorption intensity (n) values. For this system, the n numbers were found to be greater than 2. Considering that adsorption acts physically, the pace of all n is greater than 1, indicating favourable adsorption. Towards assessing the propensity for adsorption of absorbent for the adsorbed species, a Temkin isotherm plot was used. As a result of communications between the adsorbent and the adsorbate, the temperature of molecular adsorption in a layer decreases linearly with coverage. The Temkin isotherm makes the assumption that in contrast to logarithms, the heat of adsorption is linear. The linear Temkin isotherm model [23] is described below.

$$q_e = \frac{RT}{b_T} \ln a_T + \frac{RT}{b_T} \ln C_e \quad (4)$$

Where R is the universal gas constant (J K^{-1} mol^{-1}), adsorption heat is represented by b_T (kJ mol^{-1}), a_T is the symmetry binding constant (L/mg), and T is the temperature (K).

q_e and ln C_e of the Temkin isotherm are shown in Figure 3. The intercepts and slope of the C_e plot were used to obtain the Temkin constants a_T and b_T during binding constant values at equilibrium, heat of adsorption moral standards, and CRD adsorption was provided to the binding free energy and adsorption heat feasible. Table 2 displays the adsorption equilibrium data.

Table 2. Adsorption of CRD on AIBAC outcomes from isotherm models.

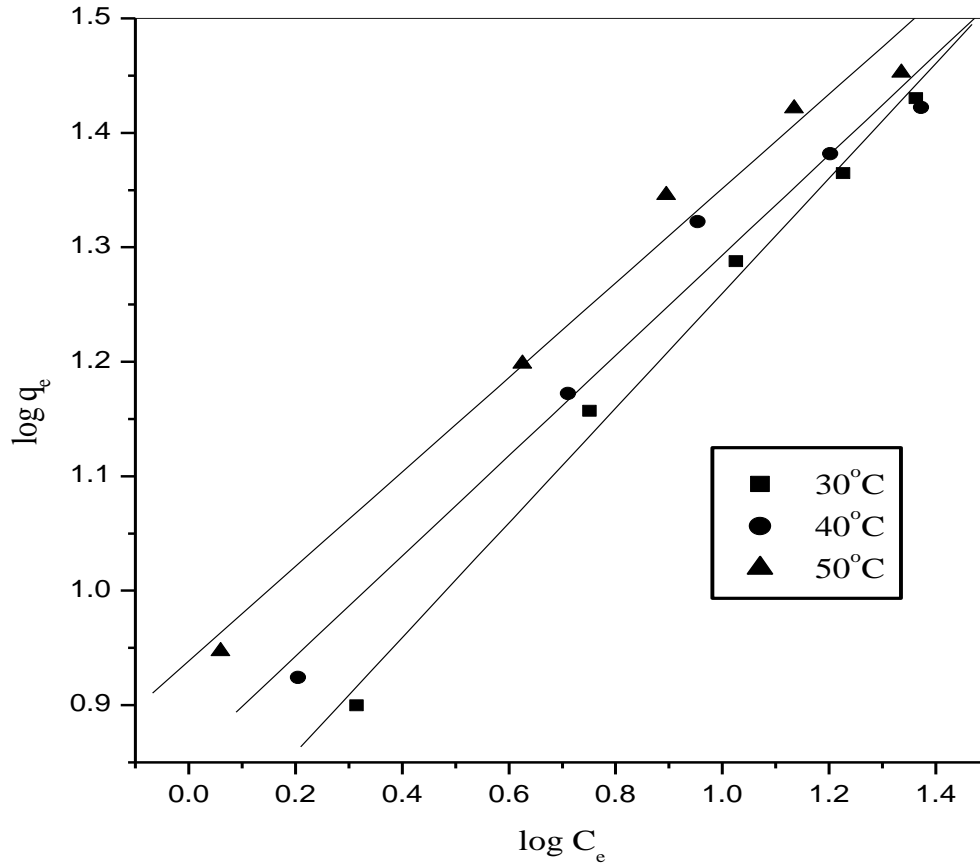| Temp. (°C)	Langmuir Isotherm			Freundlich Isotherm			Temkin Isotherm		
	Correlation coefficient	Constants		Correlation coefficient	Constants		Correlation coefficient	Constants	
	r^2	Q_0 (mg/g)	b_L (L/mg)	r^2	k_f	n	r^2	b_T (kJ mol^{-1})	a_T (L/mg)
30	0.995	35.211	0.125	0.995	5.731	1.993	0.994	17.796	1.697
40	0.998	33.444	0.198	0.987	7.163	2.283	0.993	15.923	4.801
50	0.997	31.949	0.258	0.991	8.682	2.422	0.992	16.009	7.338

Figure 1. CRD adsorption on AIBAC according to the Langmuir isotherm.
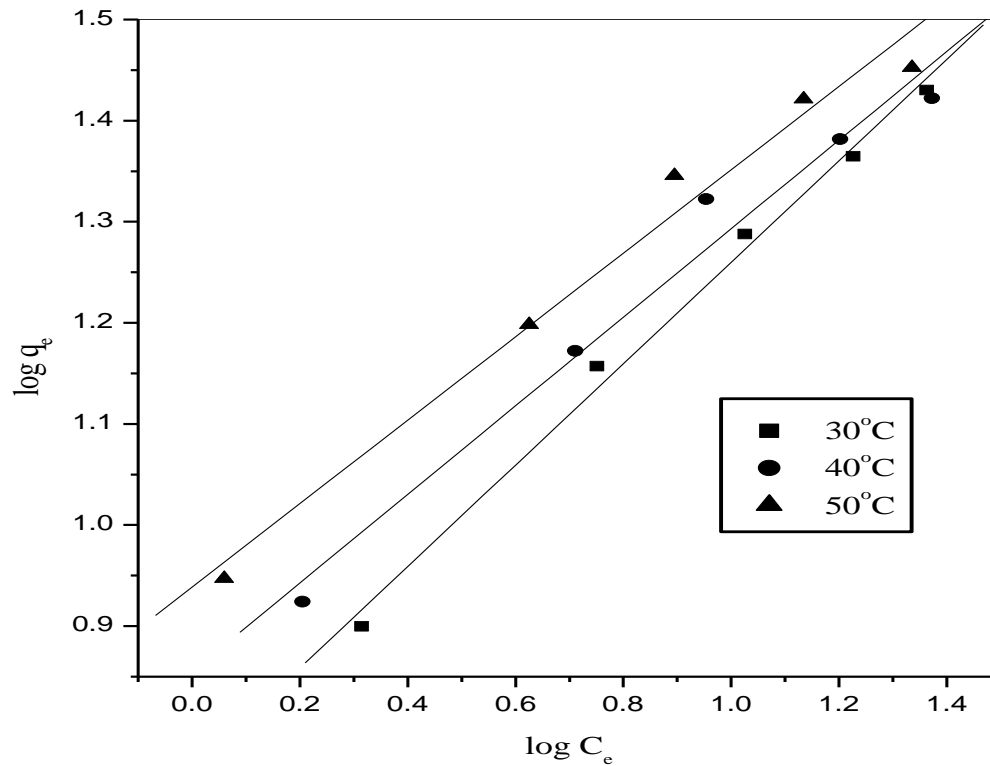
Figure 2. CRD adsorption on AIBAC according to the Freundlich isotherm.

42   A. Siva Kumar, G. Rama Chandran,
     and P. Thamilarasu

Thermodynamic, Kinetic and Equilibrium Investigation of
Activated Carbon Prepared from the Bark of *Azadirachta
indica L.* Acid Dispersion to Remove Congo Red Dye
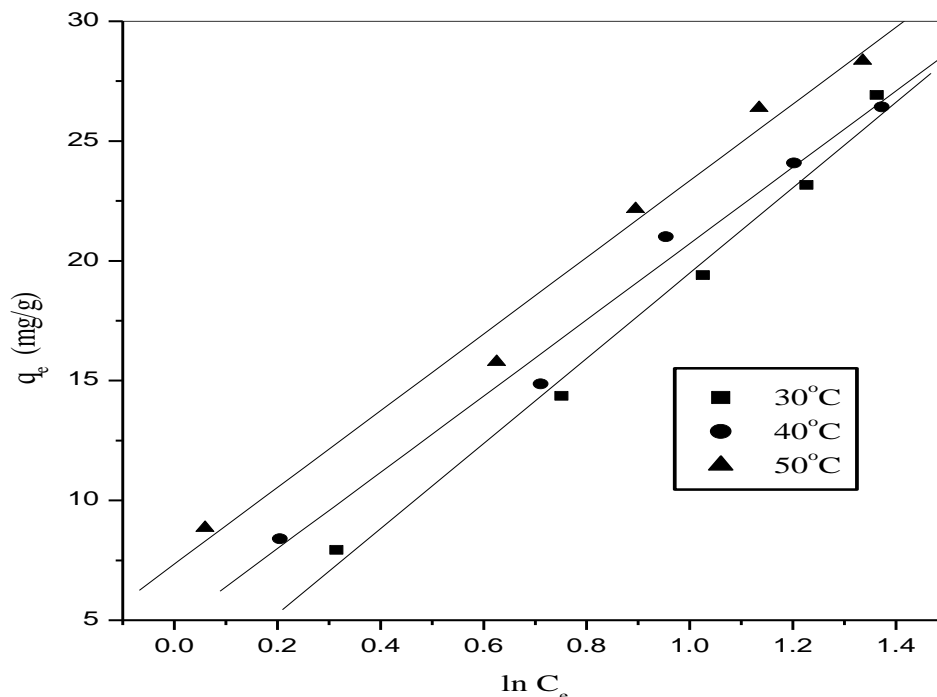
Figure 3. CRD adsorption on AIBAC according to the Temkin isotherm.

4.   Aspects of Thermodynamics

To get enthalpy change (H°), entropy change (G°), and free energy change (S°), the thermodynamic equilibrium constant (K_o) was used. According to the method described in [24], the equilibrium of the adsorption mechanism has consistent values. With both of the following equations, the fundamentals of thermo-dynamics fluctuate.

$$Ln\ K_o\ =\ \frac{\Delta S^o}{R} - \frac{\Delta H^o}{RT} \qquad (5)$$

$$\Delta G^o\ =\ - RT\ ln\ K_o \qquad (6)$$

Where, the usual adsorption enthalpy is H° (k J mol^{-1}), ΔG^o is the maximum change in limitless energy (k J mol^{-1}), and ΔS^o is the standard entropy change (J K^{-1}mol^{-1}). The values ΔH^o and ΔS^o can be obtained from the slope and intercept of the plot of ln K_o vs $\frac{1}{T}$.

Table 3 shows changes in equilibrium constant, enthalpy, entropy, and standard free energy. The findings indicated that the endothermic nature of adsorption resulted in a spike in K_o as the temperature was raised. From the observations, the initial CRD concentration increased with the standard free energy values. Standard free energy values were negative, confirming a phenomenon of spontaneous adsorption. Due to the adsorption of CRD on AIBAC, enthalpy change values between 13 and 28 kJ mol^{-1} were seen. The endothermic aspect of the physical interactions between AIBAC and CRD and the adsorption process was shown by these values. For the adsorption of CRD on AIBAC, conventional entropy values ranged from 16 to 104 J K^{-1}mol^{-1}, which are positive. The adsorption of CRD on AIBAC was found to have a high extent of contributed extensively for the solid-solution interface [25].

Table 3. Thermodynamic parameters for adsorption of CRD on AIBAC.

C_o	K_o			ΔG^o (kJ mol^{-1})			ΔH^o	ΔS^o
(mg/L)	30°C	40°C	50°C	30°C	40°C	50°C	(kJ mol^{-1})	(J K^{-1} mol^{-1})
10	3.844	5.232	7.720	-3.392	-4.306	-5.488	28.317	104.524
20	2.545	2.893	3.739	-2.353	-2.764	-3.542	15.589	59.043
30	1.831	2.337	2.825	-1.524	-2.209	-2.788	17.642	63.293
40	1.376	1.513	1.936	-0.804	-1.078	-1.774	13.818	48.043
50	1.167	1.121	1.309	-0.389	-0.296	-0.724	12.903	16.184

43   A. Siva Kumar, G. Rama Chandran,
and P. Thamilarasu

Thermodynamic, Kinetic and Equilibrium Investigation of
Activated Carbon Prepared from the Bark of *Azadirachta indica L.* Acid Dispersion to Remove Congo Red Dye

5.   Adsorption Equilibrium Investigation

The data obtained from batch experiments were reviewed using a range of kinetics models, including the models of spurious first and second categories established by Lagergren. The properties of the integrated pseudo-first order kinetic form is represented by

$$\log(q_e - q_t) = \log q_e - \frac{k_1}{2.303}t \quad (7)$$

Where q_e and q_t represent the amounts of CRD adsorbed on AIBAC at equilibrium and time t, respectively, and k_1 represents the pseudo-first order rate constant (min^{-1}).

As a result, since first order kinetics dominated the adsorption, a regular approach was anticipated between the two parameters log (q_e-q_t) and t. The values of k_1 and q_e allowed the slope and intercept of the first order plot to be evaluated. A pseudo-second order kinetic model may also be employed to explain the adsorption if first order kinetics fails to sufficiently represent it.

The pseudo-second order model's linear system representation is as the following.

$$\frac{t}{q_t} = \frac{1}{k_2 q_e^2} + \frac{1}{q_e}t \quad (8)$$

k_2 of the hypothetical second order rate is constant (g mg^{-1} min^{-1}). If the adsorption follows second order, a graph of t / qt and t should show a linear relationship, and q_e and k_2 can be obtained from the slope and intercept of the second order plot.

The kinetics data shown in Table 4 considerably depict the first order and parameters of the second order. The paradigm of spurious second order showed good agreement to the pseudo-first order rate equation of adsorption capacity between computed and experimental results. The experimental results for the adsorption of CRD in a pseudo-second order model have a good correlation coefficient ($r^2 = 0.998$) and very little relative variance in percentage terms. Based on the above-mentioned findings, the correlation for dye adsorption was obtained by the instance of a pseudo-second order model that matches a pseudo-first order model [26, 27].

The pseudo-first order kinetics for the adsorption of CRD on AIBAC is shown in Figure 4, and the adsorption of CRD on AIBAC but using a completely zero order kinetics technique is shown in Figure 5.

Table 4. Pseudo-first and second orders used to account for absorption of CRD on AIBAC.

C_o (mg/L)	q_e (exp) (mg/g)	pseudo-first order kinetic model				pseudo-second order kinetic model			
		q_e (cal) (mg/ g)	k_1 (min^{-1})	r^2	P	q_e (cal) (mg/g)	k_2 (g mg^{-1} min^{-1})	r^2	P
10	7.936	3.745	0.032	0.963	52.81	8.446	0.014	0.998	6.43
20	14.358	4.554	0.022	0.985	68.28	14.993	0.009	0.998	4.42
30	19.404	7.063	0.025	0.987	63.59	20.449	0.006	0.998	5.39
40	23.165	13.314	0.024	0.901	42.53	25.381	0.003	0.992	4.69
50	26.927	13.623	0.015	0.953	49.43	29.498	0.002	0.979	4.53

44   A. Siva Kumar, G. Rama Chandran, and P. Thamilarasu

Thermodynamic, Kinetic and Equilibrium Investigation of Activated Carbon Prepared from the Bark of *Azadirachta indica L.* Acid Dispersion to Remove Congo Red Dye
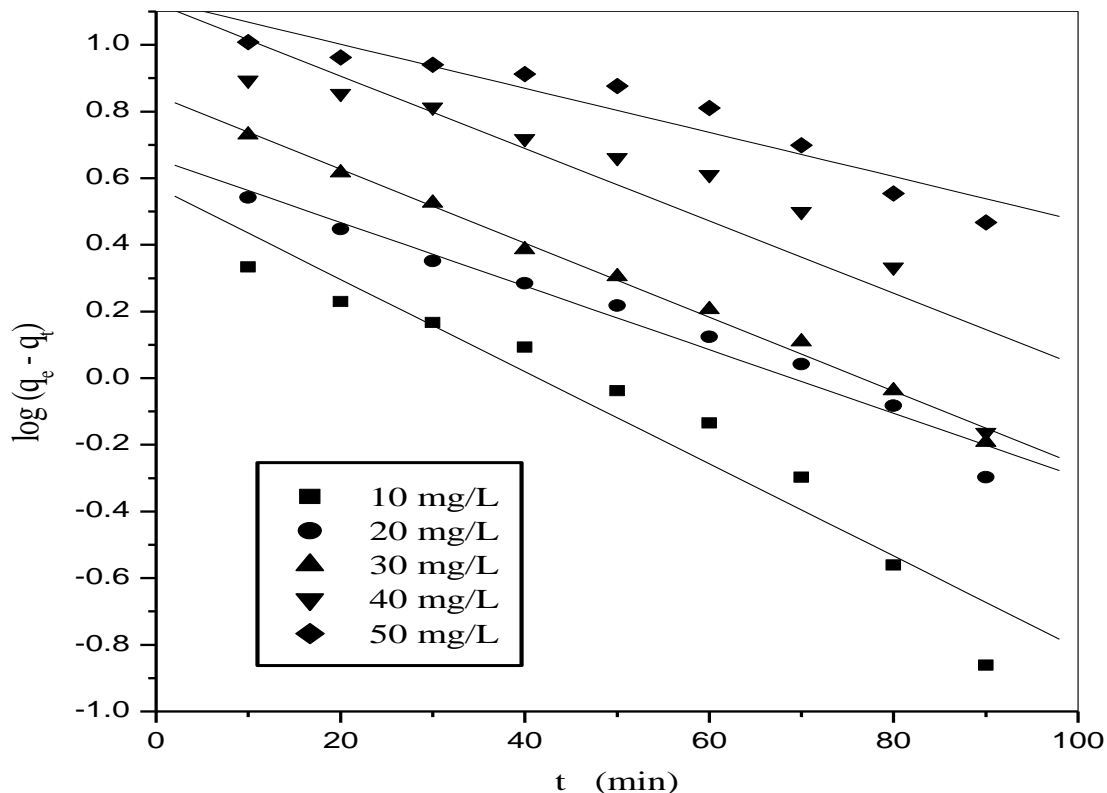

Figure 4. Pseudo-first order kinetics for adsorption of CRD on AIBAC.
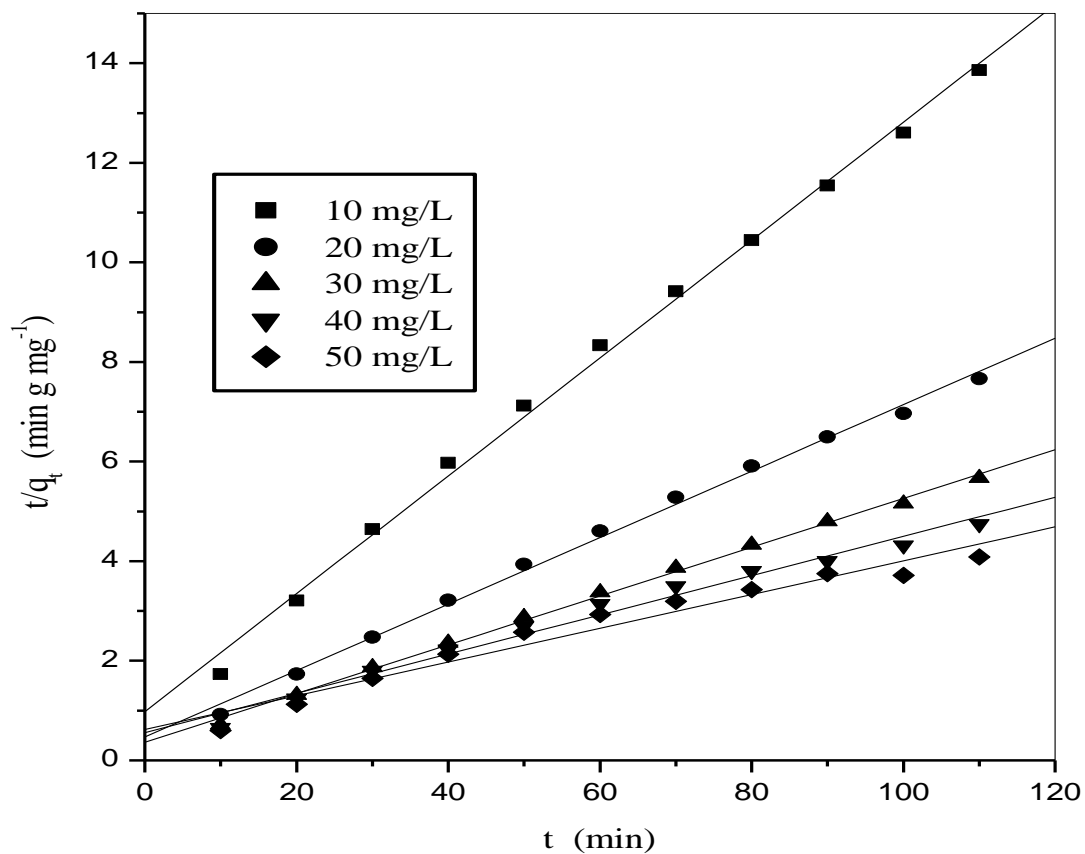
Figure 5. Adsorption of CRD on AIBAC using a completely zero order kinetics technique.

45   A. Siva Kumar, G. Rama Chandran, and P. Thamilarasu

Thermodynamic, Kinetic and Equilibrium Investigation of Activated Carbon Prepared from the Bark of *Azadirachta indica L.* Acid Dispersion to Remove Congo Red Dye

6.   Infrared Spectroscopic Fourier Transform Studies

The porosity of the nano-sorbent and the amount that can be absorbed are regulated by the functional groups at the surface and the associated chemical reactivity. Because of the imbalance between surface forces and internal pressure carried on by this reactivity, molecules are drawn towards the related entity force used. To evaluate the kind and pattern of adsorption, FT-IR spectra of AIBAC were taken before and after adsorption of CRD, which are shown in Figures 6 and 7. The peak at 3783 cm^{-1} of the AIBAC spectra showed the existence of -OH group in the adsorbent. Stretching of H-N atoms was observed at 3409 cm^{-1}, and aromatic HC atoms could be seen at 2922 and 2853 cm^{-1}, the occurrence of the -C-C triple bond in the adsorbent stretching group was indicated by a 2023 cm^{-1} peak. The carbonyl group's - O=C stretch could be seen in the area at 1704 cm^{-1}. H-N stretch of the amine group, -H-C stretch of the alkane, and -NC stretch of the aliphatic amine were all indicated in the region at 1612 cm^{-1}. The wave number range changed somewhat following the adsorption of CRD onto the adsorbent, and some wave number regions were not seen. It indicated that CRD had contributed in the adsorption of AIBAC [28].
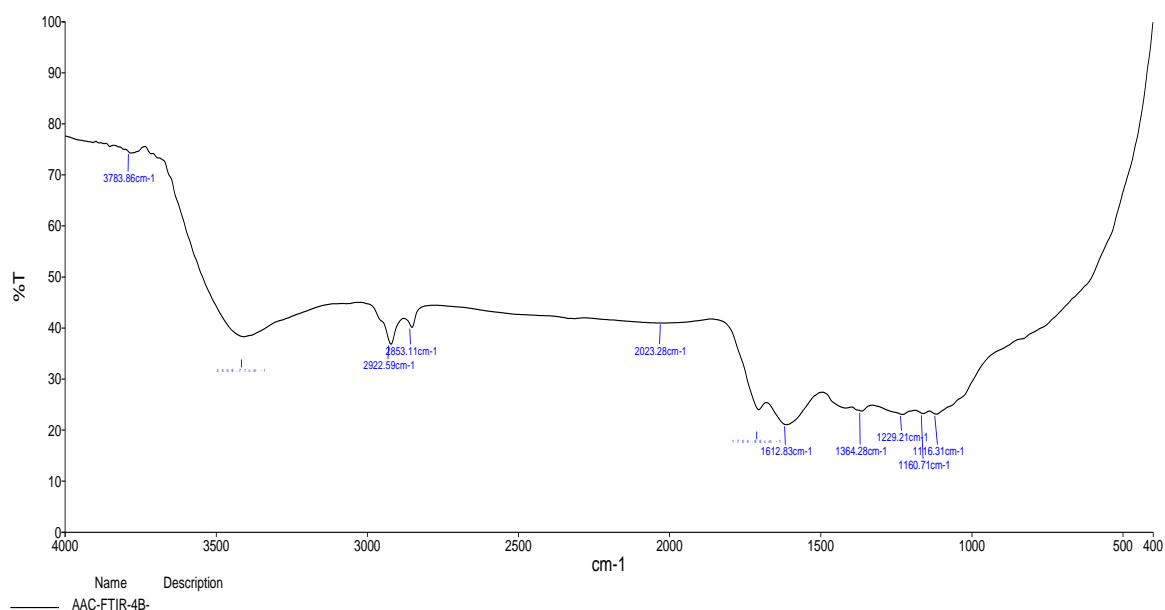

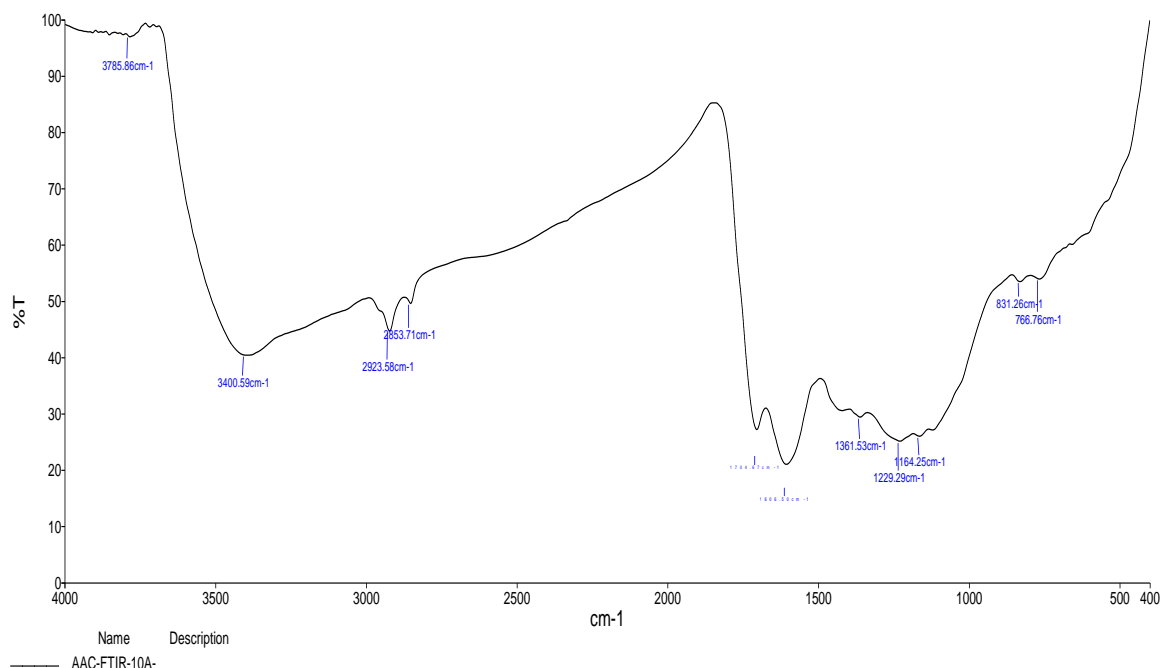**Figure 6.** FT-IR spectrum of AIBAC before adsorption of CRD on AIBAC.

Figure 7. FT-IR spectrum of AIBAC after adsorption of CRD on AIBAC.

46   A. Siva Kumar, G. Rama Chandran,
and P. Thamilarasu

Thermodynamic, Kinetic and Equilibrium Investigation of
Activated Carbon Prepared from the Bark of *Azadirachta
indica L.* Acid Dispersion to Remove Congo Red Dye

7.   Scanning Electron Microscopy (SEM) Studies

Scanning electron microscopy images before and after the adsorption of Congo red dye on AIBAC are shown in Figures 8 and 9, respectively. The images transparently demonstrated that AIBAC had a porous structure prior to adsorption. Its adsorbent surface featured pores and openings resembling caves, which might undoubtedly enhance the amount of adsorption-friendly surface area. SEM images taken subsequent to CRD adsorption showed unambiguously that CRD had adhered to the caves, pores, and surfaces of AIBAC. The images amply demonstrated that the adsorption of CRD altered the structure of AIBAC [29].
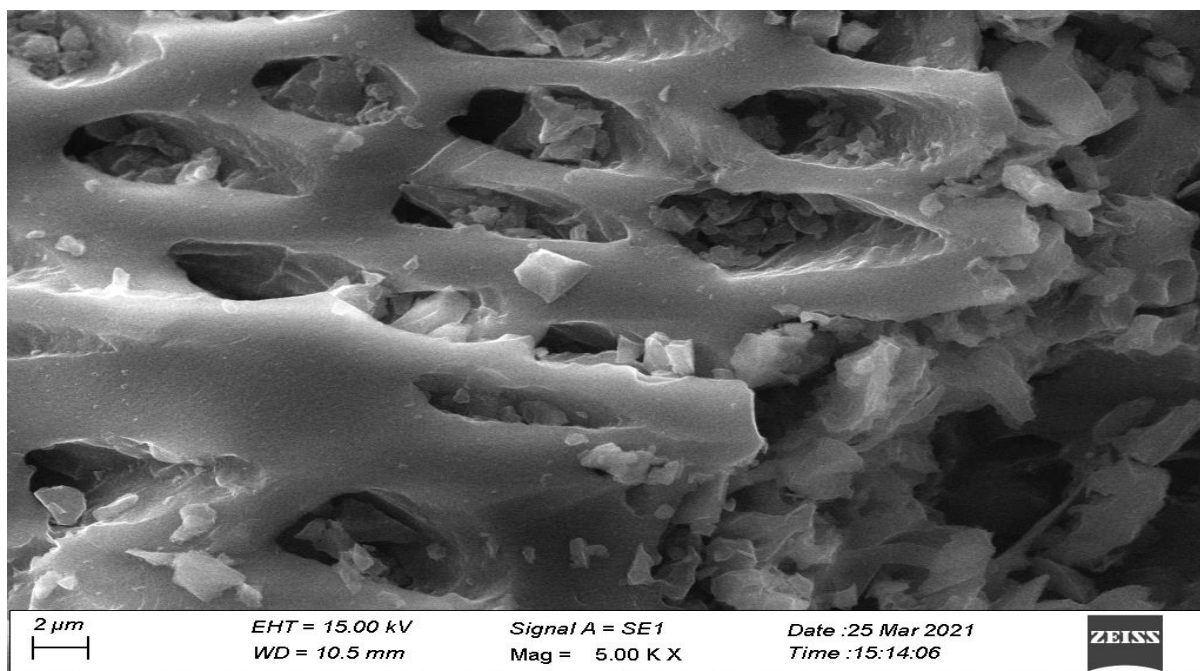
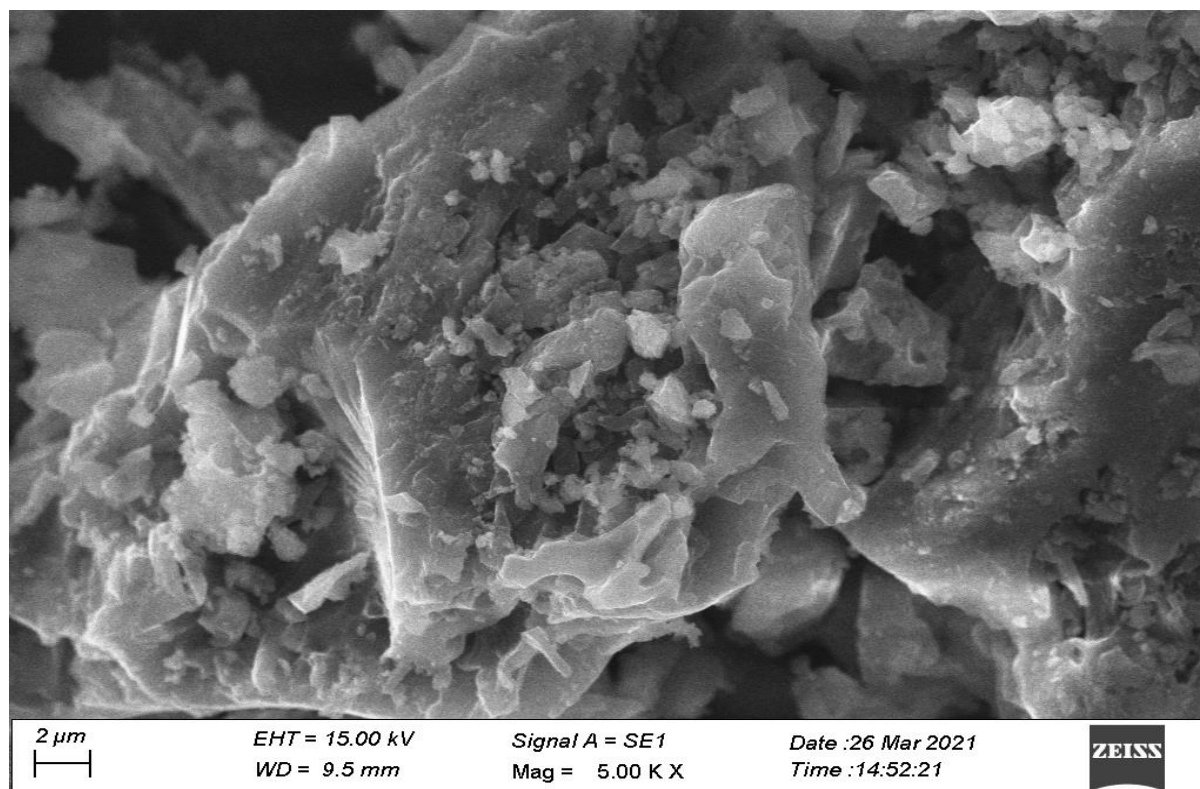**Figure 8.** SEM photograph before adsorption of CRD on AIBAC.

Figure 9. SEM photograph after adsorption of CRD on AIBAC.

47   A. Siva Kumar, G. Rama Chandran, and P. Thamilarasu

Thermodynamic, Kinetic and Equilibrium Investigation of Activated Carbon Prepared from the Bark of *Azadirachta indica L.* Acid Dispersion to Remove Congo Red Dye

CONCLUSION

The *Azadirachta indica* L. Bark Activated Carbon (AIBAC), a readily available, environmentally acceptable, and reasonably priced material, is capable of being utilised as an adsorbent to remove CRD from aqueous solutions. The solution's optimum pH is 5.0, the ideal contact period is 100 minutes, and the recommended adsorbent dosage for the elimination of CRD is 100 mg. The adsorption capabilities of AIBAC-CRD are by the adsorption isotherm models presented. FTIR and SEM tests were used to describe the adsorption of CRD. Comparable to the kinetic model of pseudo-first order, there is a stronger agreement with the kinetic system of pseudo-second order. The amount of CRD that was eliminated increased as the temperature increased from 30° C to 50° C.

ACKNOWLEDGEMENT

REFERENCES

1. Raghuvanshi, S. P., Singh, R., Kaushik, C. P., Raghav, A. K. (2005) Removal of textile basic dye from aqueous solutions using sawdust as bio-adsorbent. *International Journal of Environmental Studies*, **62**, 329–339.

2. Allen, S. J., Mckay, G., Porter, J. F. (2004) Adsorption isotherm models for basic dye adsorption by peat in single and binary component systems. *Journal of Colloid Interface Science*, **280**, 322–333.

3. Kuo, W. G. (1992) Decolourizing dye waste water with Fenton reagent. *Water Research*, **26**, 881–886.

4. Walsh, G. E., Bahnes, L. H., Horning, W. B. (1980) Toxicity of textile mill effluents to fresh water and estuarine algae, Crustaceans and fishes. *Environmental Pollution*, **A21**, 169–179.

5. Sadeghfar, F., Ghaedi, M., Zalipour, Z. (2021) Chapter 4 - Advanced oxidation, Editor(s): Mehrorang Ghaedi, *Interface Science and Technology*, **32**, 225–324.

6. de Brito, J. F., Bessegato, G. G., e Souza, P. R. F., Viana, T. S., de Oliveira, D. P., Martínez-Huitle, C. A., Zanoni, M. V. B. (2019) Combination of Photoelectrocatalysis and Ozonation as a Good Strategy for Organics Oxidation and Decreased Toxicity in Oil-Produced Water. *Journal of Electrochemical Society*, **166**, H3231.

7. Chen, L., Xu, Y., Sun, Y. (2019) Combination of Coagulation and Ozone Catalytic Oxidation for Pretreating Coking Wastewater. *International Journal of Environmental Research and Public Health*, **16**, 1705. doi: 10.3390/ijerph16101705.

8. Mecha, A. C., Chollom, M. N. (2020) Photo-catalytic ozonation of wastewater: a review. *Environmental Chemistry Letters*, **18**, 1491–1507.

9. Hasnain, I. M., Siew, L. L., Asaari, F. A. H., Aziz, H. A., Azam, R. N., Dhas, J. P. A. (2007) Low cost removal of disperse dyes from aqueous solution using palm ash. *Dyes Pigments*, **74**, 446– 453.

10. Namasivayam, C., Kumar, M. D., Kumar, S., Begum, R. A., Vanathi, T., Yamuna, R. T. (2001) Waste coir pith — a potential biomass for the treatment of dyeing waste water. *Biomass Bioenergy*, **21**, 477–483.

11. Rajeshwari, S., Subburam, V. (2002) Activated parthenium carbon as an adsorbent for the Removal of dyes and heavy metal ions from aqueous solution. *Bioresource Technology*, **85**, 205–206.

12. Lata, H., Garg, V. K. Gupta, R. K. (2007) Removal of basic dye from aqueous solution by Adsorption using *Parthenium hysterophorus*: An agricultural waste. *Dyes Pigments*, **74**, 753–758.

13. Khattri, S. D., Singh, M. K. (1999) Colour removal from dye wastewater using sugar cane dust as an adsorbent. *Adsorption Science Technology*, **17**, 269– 282.

14. Ozacar, M., Sengil, A. I. (2005) Adsorption of Meta complex dye from aqueous solution by Pine sawdust. *Bioresource Technology*, **96**, 791–795.

15. Vasanth, K., Sivanesan, S. (2007) Isotherms for Malachite Green on rubber wood (*Hevea brasiliensis*) sawdust: Comparison of linear and non-linear methods. *Dyes Pigments*, **72**, 124–129.

16. Gupta, V. K., Mittal, A. L., Krishnan, L., Mittal, J. (2006) Adsorption treatment and recovery of the hazardous dye, Brilliant Blue FCF, over bottom ash and deoiled soya. *Journal of Colloid Interface Science*, **293**, 16–26.

17. Jumasiah, A., Chuah, T. G., Gimbon, J., Choong, T. S. Y. Azni, I. (2005) Adsorption of basic dye on palm kernel shell activated carbon: sorption equilibrium and kinetics studies. *Desalination*, **186**, 57–64.

48   A. Siva Kumar, G. Rama Chandran,
     and P. Thamilarasu

Thermodynamic, Kinetic and Equilibrium Investigation of
Activated Carbon Prepared from the Bark of *Azadirachta
indica L.* Acid Dispersion to Remove Congo Red Dye

18. Mittal, A. (2006) Adsorption kinetics of removal of a toxic dye, Malachite green, from wastewater using hen feather. *Journal of Hazardous Materials*, **133**, 196–202.

19. Bello, O. S., Ahmad, M. A. (2011) Adsorptive removal of a synthetic textile dye using cocoa pod husks. *Toxicological and Environmental Chemistry*, **33**, 1298–1308.

20. Foo, K. Y., Hameed, B. H. (2011) Preparation of activated carbon from date stones by microwave induced chemical activation: Application for methylene blue adsorption. *Chemical Engineering Journal*, **170**, 338–341.

21. Hameed, B. H., Mahmoud, D. K., Ahmad, A. L. (2008) Equilibrium modelling and kinetics studies on the adsorption of basic dye by a low-cost adsorbent: coconut (*Cocos nucifera*) bunch waste. *Journal of Hazardous Materials*, **158**, 65–72.

22. Langmuir, I. (1916) The constitution and fundamental properties of solids and liquids. Part I. Solids. *The Journal of the American Chemical Society*, **38**, 2221–2295.

23. Treybal, R. E. (1981) Mass-Transfer Operation, McGraw-Hill, New York, USA, 3rd edition.

24. Elovich, S. Y., Larinov, O. G. (1962) Theory of adsorption from solutions of nonelectrolytites on solid adsorbents(I) equation adsorption isotherm from solutions and the analysis of its simplest from, (II) verification of the equation of adsorption isotherm solution. *Izvestiya AkademiiNauk SSSR*, **2**, 209–216.

25. Stephen Inbaraj, B., Sulochana, N. (2002) Basic dye adsorption on a low cost carbonaceous sorbent-kinetic and equilibrium studies. *Indian Journal of Chemical Technology*, **9**, 201–208.

26. Alshabanat, M., Alsenani, G., Almufarij, R. (2013) Removal of Crystal Violet Dye from Aqueous Solutions onto Date Palm Fiber by Adsorption Technique. *Journal of Chemistry*, Article ID 210239, 1–6.

27. Ho, Y. S., Mckay, G. (1998) Sorption of dye from aqueous solution by peat. *Chemical Engineering Journal*, **70**, 115–124.

28. Sricharoenchaikul, V., Pechyen, C., Aht-ong, D., Atong. D. (2008) Preparation and characterization of activated carbon from the pyrolysis of Physic nut (*Jatrophacurcas*L) waste. *The Journal of the American Chemical Society*, **22***, 31–37.

29. Gopinathan, R., Bhowal, A., Garlapati, C. (2017) Adsorption Characteristics of Activated Carbon for the reclamation of coloured effluents containing Orange G and New Solid-Liquid phase Equilibrium Model. *Journal of Chemical and Engineering Data*, **62**, 558–567.